Prestack Kirchhoff migration

Kangan Fang

ABSTRACT

Conventional NMO + Stack processing does not work well in structurally complex areas. Especially in the case of converted waves, true CCP stacking is not always achievable in such areas. Therefore, prestack migration is a preferred alternative. In this paper, some aspects of prestack Kirchhoff migration are reviewed and test results for both P-P data and P-SV data are presented. It turns out that the Kirchhoff algorithm migrates both P-P data and P-SV data very accurately.

INTRODUCTION

In an area of complex substructure, it is difficult to obtain a high quality stack section. Hence, the quality of poststack migration is poor. A good way to solve this problem is prestack migration. There are many prestack migration algorithms available. The Kirchhoff method is one of the best methods to do prestack migration. It is easy to implement, can handle dips up to 90˚, and is accurate in a medium with only vertical velocity variations.

PRESTACK KIRCHHOFF MIGRATION

As illustrated in Figure 1, we assume that every point in the subsurface is a scatter point which scatters waves coming from a source point S. The wavefield collected at the Earth's surface is a superposition of waves coming from every scatter point. In migration, we propagate the surface wavefield back to subsurface scatter points and collect wavefield at $t = 0$ to get the image of subsurface structure.

Let $P(x_s, x_r, z = 0)$ be the wavefield at the Earth's surface. The wavefield at every scatter point is :

$$P(x,z,t) = \int A\left(\frac{\partial}{\partial t}\right)^{\frac{1}{2}} P\left(x_s, x_r, z = 0, t + \frac{r_s}{v_d} + \frac{r_r}{v_u}\right) dx_s dx_r \qquad (1)$$

where, x_s and x_r are the x coordinates of source and receiver, respectively; r_s and r_r are the travel distances from source to scatter point and from scatter point to receiver, respectively; v_d and v_u are the velocities of downgoing and upgoing raypaths, respectively.

$$A = \frac{\cos(\theta_s)\cos(\theta_r)}{\sqrt{v_d v_u r_s r_r}} \qquad (2)$$

is the amplitude scale factor.

So the image of the subsurface is represented by :

$$P(x,z) = \int A\left(\frac{\partial}{\partial t}\right)^{\frac{1}{2}} P\left(x_s, x_r, z=0, \frac{r_s}{v_d} + \frac{r_r}{v_u}\right) dx_s dx_r \qquad (3)$$

For P-P wave data migration, let $V_d = V_u = V_p$;

For P-SV wave data migration, let $V_d = V_p$ and $V_u = V_s$;

Here V_p is the P-wave velocity and V_s is the S-wave velocity.

Therefore, we can conclude that Kirchhoff migration is fairly easy to implement and the same program can be used to migrate both P-P waves and converted waves.

IMPLEMENTATION

The migration is performed on shot gathers. Each gather is read in and its contribution is added to each scatter point at the output traces. In the implementation of Kirchhoff migration, several aspects should be taken in account, including phase and amplitude adjustments, aliasing reduction, and dip angle limitation. Equation (2) is used as the amplitude compensation, which gives reasonable results. Because Kirchhoff summation is performed both in source and receiver dimension, we must consider the aliasing caused by the undersampling in both dimensions. Here, for migration performed on shot gathers, the aliasing is much more severe than aliasing in CMP gathers. One method is performing interpolations in both dimensions. Limiting the range of angles θ_s and θ_r (Figure 1) can filter out dips of events which are not desired.

IMPULSE RESPONSE

For a P-P wave, the impulse response of the prestack migration is an ellipse, as shown in Figure 2.

For a P-SV wave, the impulse response is a distorted ellipse. The right side of the ellipse is squeezed in, as shown in Figure 3.

For an SV-P wave, the impulse response is also a distorted ellipse. But in this case, the left side of the ellipse is squeezed in, as shown in Figure 4.

The distortion of the impulse ellipse is caused by the asymmetry of the velocity function along the downgoing and upgoing paths of the waves and this can be explained by Fermat's principle.

SYNTHETIC DATA TEST RESULTS

Two models were created to test the migration algorithm described above. Figure 5 shows a model with four layers, the third interface of the model being a triangular structure. The base angles of the triangular structure are 20˚ and 15˚, respectively. P-P wave data were created from this model and the migration result is shown in Figure 6. The triangular structure is accurately positioned.

Figure 7 shows a three-layer model. A prestack P-SV wavefield has been generated using the GXII software. The migration result is shown in Figure 8. The migration is

quite accurate. As long as large enough offsets are included and the migration aperture is reasonable, a good result can be obtained.

CONCLUSIONS AND FUTURE SUGGESTIONS

The results of tests of the prestack Kirchhoff migration are satisfactory. The Kirchhoff migration method is suitable for prestack migration of both P-P wave data and converted wave data. In order to get it to work on the real data, field data testing is needed.

ACKNOWLEDGMENT

I gratefully thank Shaowu Wang for helping me create the model data and introducing me to the use of the ITA software package, and the CREWES sponsors for their financial support.

REFERENCES FOR GENERAL READING

Li, Z. and Lynn, W., 1991, Enhancements to prestack frequency-wavenumber (*f-k*) migration: Geophysics, 56, 27-40.

Chun, J. and Jacewitz, C., 1978, A fast multi-velocity function frequency domain migration: Presented at the 48th Ann. Internat. Mtg., Soc. Expl. Geophys.

Shurtleff, R. N., 1984, A prestack *f-k* procedure for prestack migration and migration velocity analysis: Presented at the 46th Mtg., Europ. Assn. Expl. Geophys.

Bancroft, J., 1995, A practical understanding of migration and dip moveout: Lecture Note, Dept. of Geology and Geophysics, The University of Calgary.

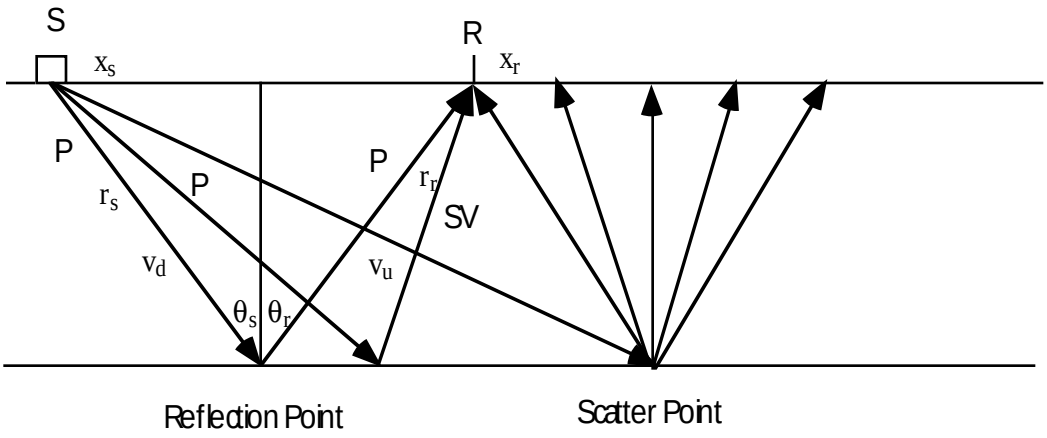

Figure 1. Illustration of shot gather and scatter points.

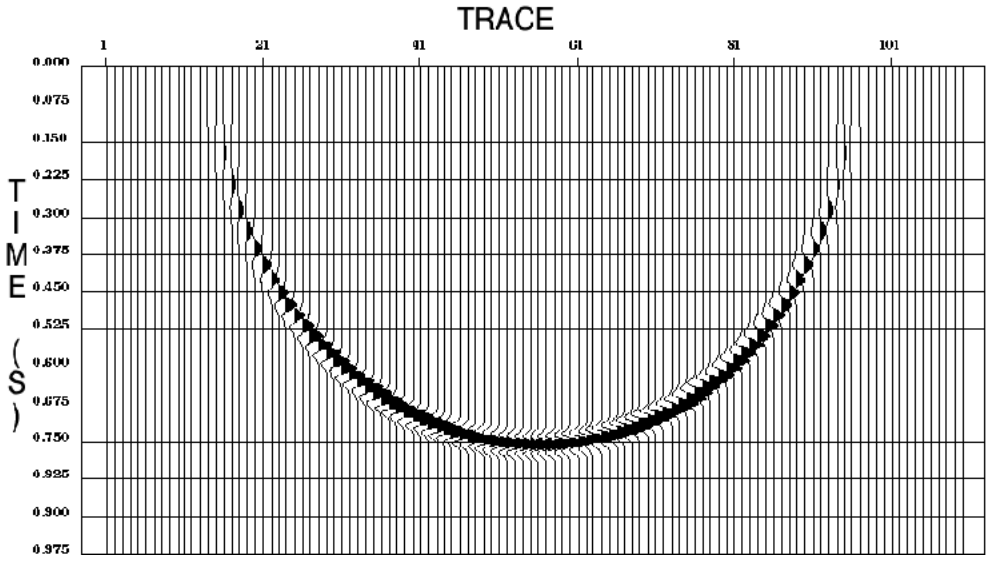

Figure 2. Impulse response of prestack migration for P-P wave.

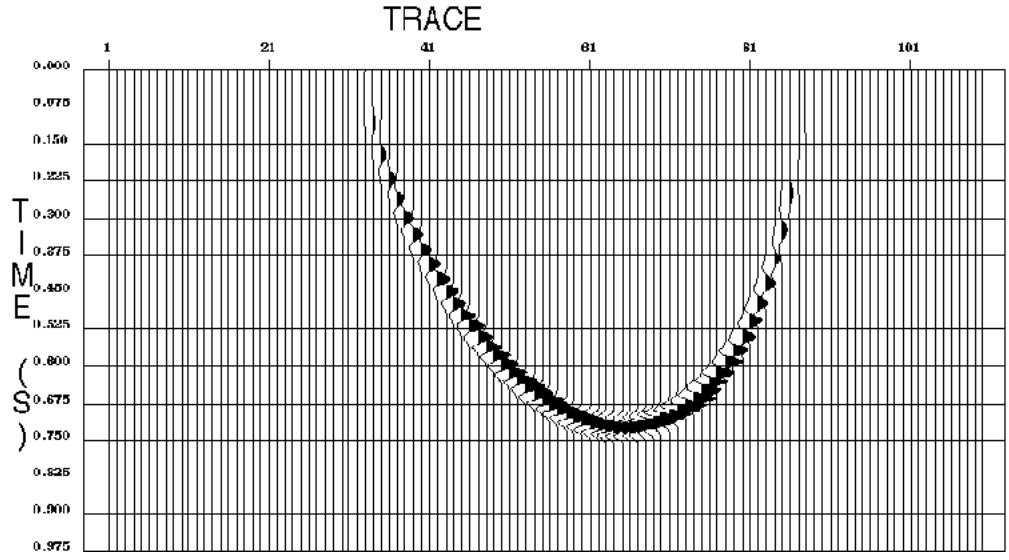

Figure 3. Impulse response of prestack migration for P-SV wave.

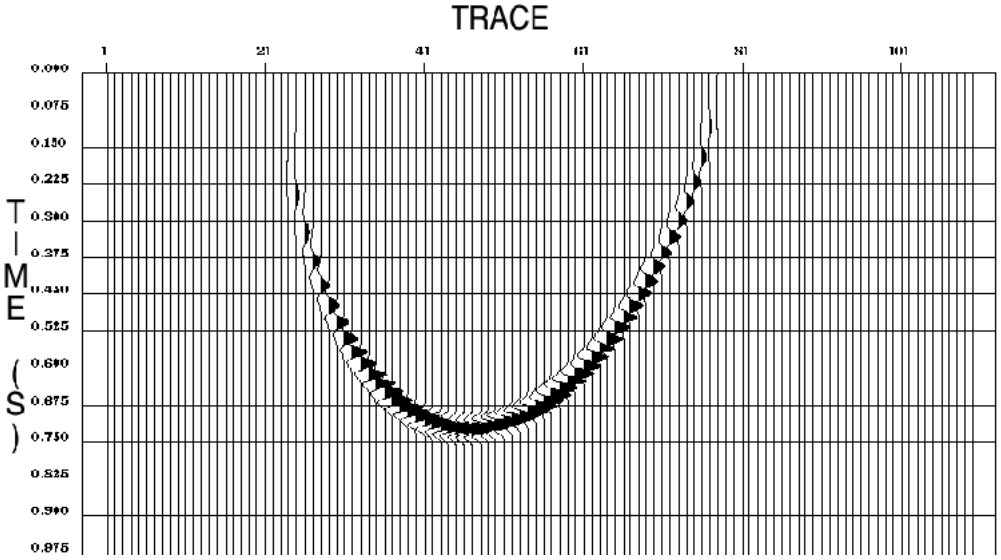

Figure 4. Impulse response of prestack migration for SV-P wave.

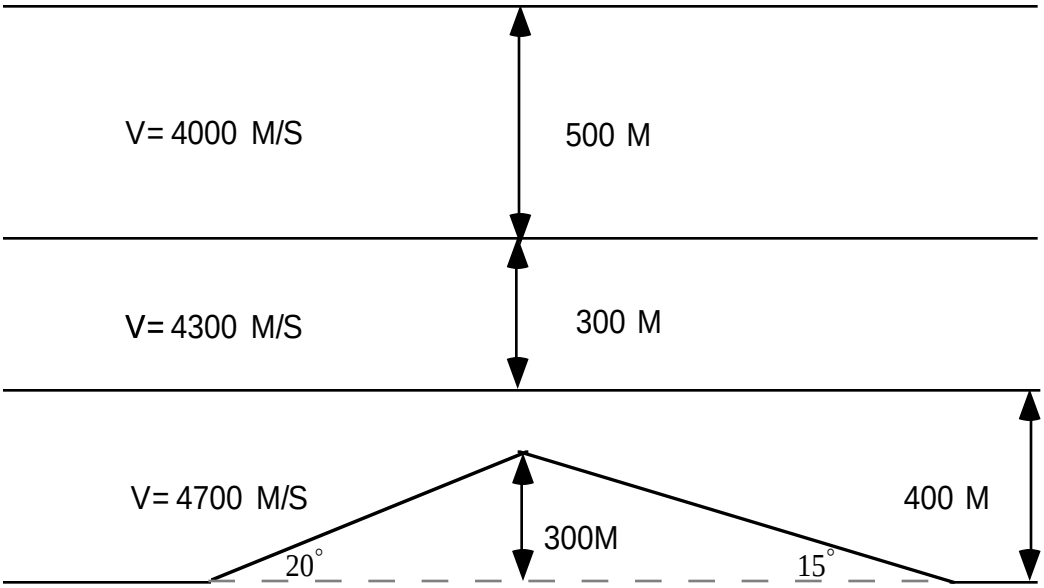

Figure 5. Model used to test migration for P-P wave.

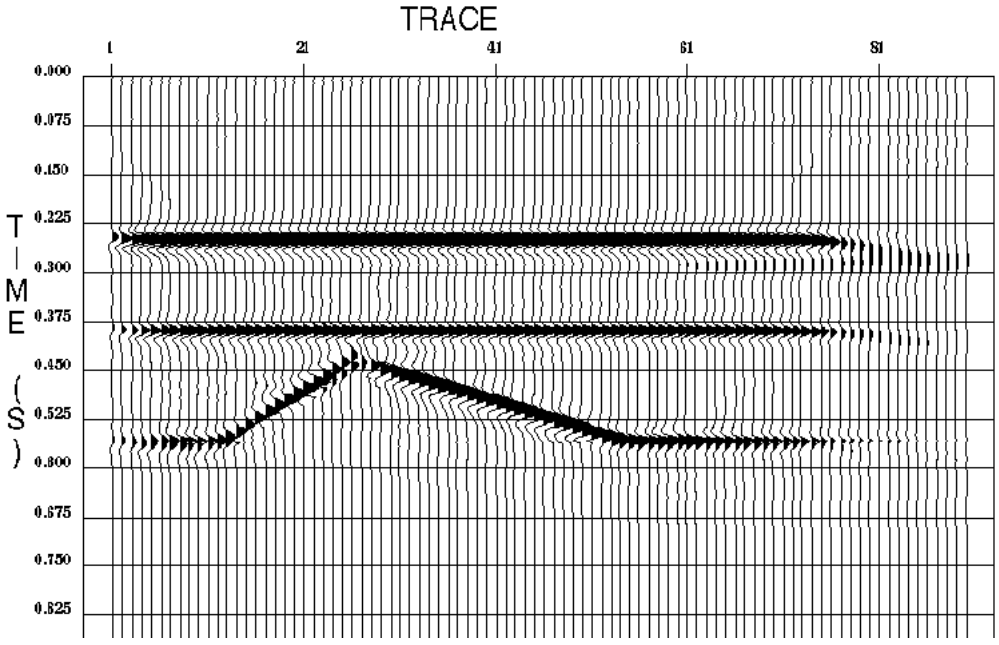

Figure 6. Migration result of P-P wave generated from model shown in Figure 5.

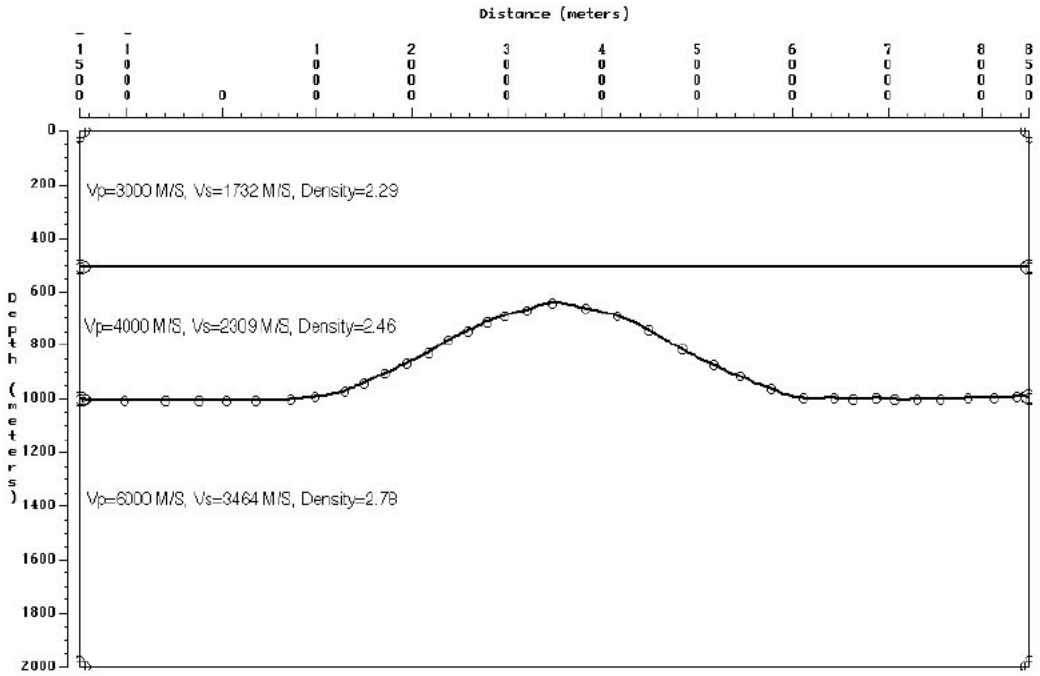

Figure 7. Model used to test migration for P-SV wave.

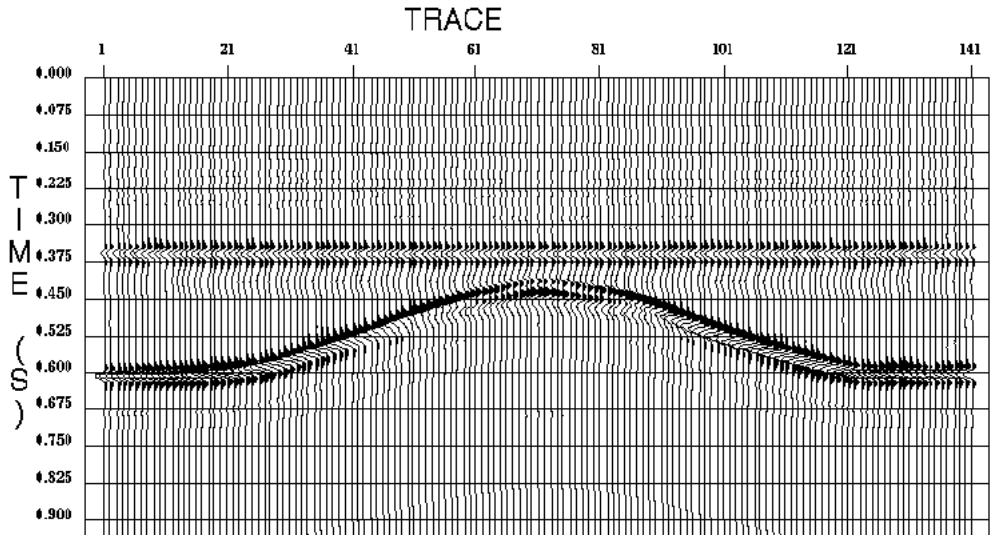

Figure 8. Migration result of P-SV wave generated from model shown in Figure 7.